Environ Geol (2007) 52:1365–1374
DOI 10.1007/s00254-006-0579-4

ORIGINAL ARTICLE

Arsenic adsorption on nanocrystalline goethite: the natural example of bolar earths from Mt Amiata (Central Italy)

A. Manasse · C. Viti

Received: 20 July 2006 / Accepted: 1 November 2006 / Published online: 1 December 2006

Abstract Bolar earths deposits from Mt Amiata (Central Italy) consist of nanosized pseudo-spherical goethite, with average crystal size of 10–15 nm (as determined by X-ray powder diffraction and transmission electron microscopy observations), possibly associated to amorphous silica and minor sheet silicates, quartz and feldspars. Chemical analyses revealed high As contents (up to 7.4 wt% As_2O_5), thus indicating the occurrence of a potentially dangerous contaminant. Arsenic doesn't occur as a specific As phase, but it is strictly associated with goethite nanocrystals. Eh and pH measurements suggest that As occurs as arsenate anions ($H_2AsO_4^-$ and $HAsO_4^{2-}$), which are easily and strongly adsorbed to goethite surfaces. The high specific surface area, resulting from goethite nanosize, and the absence of competitive anions explain the extremely efficient adsorption of arsenate and the anomalously high As content in bolar earths. Overall physical/chemical data suggest stable arsenate adsorption, with very limited risk for As release to the environment.

Keywords Bolar earths · Arsenic · Adsorption · Goethite nanocrystals · Mt Amiata

A. Manasse · C. Viti (✉)
Dipartimento di Scienze della Terra,
University of Siena, Siena, Italy
e-mail: vitic@unisi.it

A. Manasse
e-mail: manasse@unisi.it

Introduction

Arsenic is a widespread contaminant, dangerous to metabolic processes and responsible for serious health risks in case of high-level exposures (Smedley and Kinniburgh 2002). Arsenic concentrations exceeding the standard limits (10 μg/l As in drinking waters, according to the World Health Organization) may arise from rocks/minerals dissolution under weathering and hydrothermal conditions, geothermal activity, and several anthropogenic sources including mine wastes, smelter drainage waters, coal ash and arsenical fertilizers or pesticides (Manning et al. 1998; Garcia-Sanchez et al. 2002).

In natural systems, arsenic may occur in four oxidation states (–3, 0, +3 and +5). Prevalent species in soils and groundwaters are arsenate and arsenite, usually with the latter more mobile and toxic than the former. Arsenate is stable in a wide range of pH and Eh conditions (Smedley and Kinniburgh 2002), thus representing the most common species in natural environments.

Arsenate has strong affinity for iron oxides/hydroxides surfaces, such as hematite, goethite and ferrihydrite, that are important constituent of soils and sediments (Hiemstra and Van Riemsdijk 1999; O'Reilly et al. 2001). The adsorption mechanism on iron (hydr)oxide surfaces mostly depends on pH, which controls both the kind of anions in the solution (e.g. $H_2AsO_4^-$ and $HAsO_4^{2-}$, able to bind to surface groups by ligand exchange reactions), and the attractive/repulsive electrostatic interactions with the charged (hydr)oxide surfaces (Dzombak and Morel 1990; Hiemstra and Van Riemsdijk 1999; O'Reilly et al. 2001; Dixit and Hering 2003). Arsenic oxidation state, coordination number

and other bonding details have been determined by different spectroscopic investigations (e.g. IR and EXAFS; Waychunas et al. 1995; Sun and Doner 1996; Fendorf et al. 1997; Grossl et al. 1997; Sherman and Randall 2003).

Sediments and soils, hence, play an important role in arsenic cycling acting as either sources or sinks, depending on the prevailing geochemical environmental conditions (pH, redox potential, presence and type of adsorbing surfaces and competing anions; Gräfe et al. 2001). Arsenic is a minor but persistent constituent of other geogenic occurrences, such as volcanic gases and geothermal waters throughout the world, as well as a major constituent of sulphides and arsenides (Smedley and Kinniburgh 2002; Webster and Nordstrom 2003). However, high levels are usually associated with anthropogenic sources, such as mine-tailing ponds and acid mine drainage waters (Carlson et al. 2002); in these cases, sorption onto iron (hydr)oxides is fundamental in controlling As solubility, leaching and possible release.

An example of natural geogenic deposit with anomalously high As contents is represented by bolar earths, i.e. fine-grained, goethite-rich deposits from Mt Amiata (Central Italy). In particular, previous studies on samples from the Natural History Museum of the Accademia dei Fisiocritici of Siena revealed arsenic contents as high as 10.9 wt%, with average value of 5.6 wt% As_2O_5 (Manasse and Mellini 2006). Bolar earths thus represent one of the most efficient natural sink for As, formed in favourable physical and geochemical conditions. In order to understand the possible genetic mechanism and the reasons for such a high As content, we have performed a detailed field study, focussing both on bolar earth deposits and on possible still active deposition sites.

Geological background and arsenic distribution

Mt Amiata is a volcanic complex formed in two different phases dated back to 300 and 200 ky (Fig. 1); the first volcanic phase corresponds to the emplacement of a basal trachydacitic complex, whereas the second phase corresponds to trachyte-latite domes and lava flows with progressive episodes from SW to NE (Ferrari et al. 1996). After the main volcanic activity, Mt Amiata underwent hydrothermal activity, still active today at both ends of the SW–NE main fissure, with the geothermal fields of Bagni S. Filippo and Bagnore. The geothermal fields of Bagnore and Piancastagnaio (Fig. 1) are currently drilled and exploited by the ENEL Company (Minissale et al. 1997; Brogi 2004).

Several heavy metals (in particular, Hg and As) were mobilized during hydrothermal activity, producing important metal/sulphide mineralizations; among these, mercury and cinnabar, associated with minor realgar (AsS) and orpiment (As_2S_3), were widely exploited in the twentieth century (Cuteri and Mascaro 1995).

Therefore, Mt Amiata may host As or As-bearing phases in sediments, soils, air, drinking waters and groundwaters, arising from both anthropogenic and geogenic sources. For instance, some cold springs have arsenic amounts close to the limit value of 10 μg/l (Minissale et al. 1997; Mantelli et al. 1999; Tamasi and Cini 2004). Geochemical maps of heavy metals in stream sediments (Protano et al. 1998) indicate several arsenic anomalies in the southern and eastern sides of Mt Amiata (Fig. 1); these anomalies have been interpreted as due to anthropogenic pollution from the nearby mining sites of Abbadia S. Salvatore and Piancastagnaio, exploited for Hg-rich mineralizations. Similarly, As traces in air are due to ENEL geothermal power plants (Loppi 2000).

Notwithstanding the preferential occurrence of As-bearing mineralizations in the eastern mining district, the highest arsenic anomalies in stream sediments (up to 500 ppm; Protano et al. 1998) have been detected at the opposite side of the volcano, close to three historically important quarries of bolar earths (Fig. 1). These sediments were formed by precipitation from iron-rich fluids (Lotti 1910; Manasse 1915), outflowing at the contact between porous trachyte and underlying impermeable clays; the iron-rich fluids flooded into topological depressions, with subsequent iron (hydr)oxides flocculation, possibly assisted by biological processes (Lotti 1910; Manasse 1915).

Bolar earths deposits and samples description

Bolar earths quarries (''Cava delle Mazzarelle,'' ''Cava della Sega'' and ''Cava del Pino''; hereafter CM, CS and CP, respectively) were extensively exploited in the nineteenth and twentieth centuries for the production of yellow *raw sienna* and red *burnt sienna* pigments (Manasse 1915; Manasse and Mellini 2006). The CM quarry is now completely filled by spring water, thus avoiding any possible recognition of the originary deposit. Before exploitation, the deposit was up to 13 m thick and consisted of yellow-brown layered iron oxyhydroxides (Lotti 1910). Present samples have been collected on the lake banks; CM1 and CM2 are homogeneously

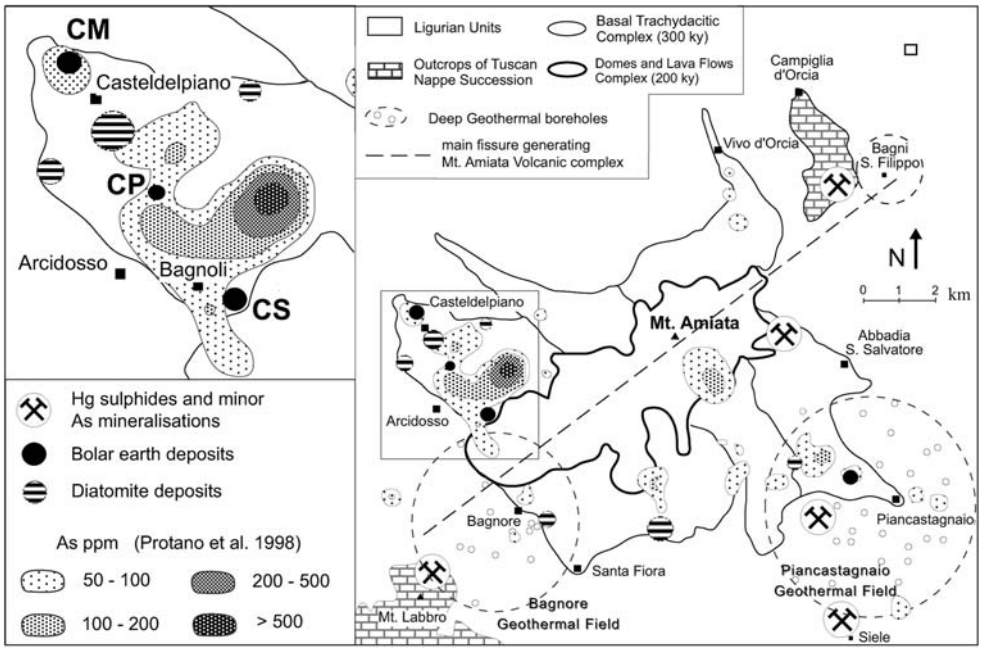

Fig. 1 Simplified geological map of the Mt Amiata Volcano, showing main mining sites, active geothermal fields, diatomite deposits and As distribution in stream sediments. CM, CP and CS are bolar earths quarries. Geological sketch modified from Brogi (2004); arsenic distribution from Protano et al. (1998)

deep-yellow and coherent, whereas CM3 is poorly coherent, with deep-yellow grains intermixed to other sediments, probably arising from trachyte weathering.

The CS quarry still shows large amounts of pure bolar earths, as well as several traces of different in situ treatments (e.g. drying areas, sieving pools, filters for raw materials sorting, ovens for the yellow-goethite to red-hematite transformation). Sample CS1 is pale-yellow, incoherent, CS2 corresponds to a dark-brown layer, whereas CS3 has been collected within a homogeneous deep-yellow, coherent layer. Preserved bolar earths are definitely rare in the CP quarry; CP1, CP2 and CP3 correspond to mixed samples, with yellow-brown grains associated with abundant sediments arising from trachyte weathering.

In order to check the possible occurrence of present-day deposition sites, we also sampled the reddish springs from Bagnoli (Fig. 1; W_{B1} and W_{B2}), the stream water flowing towards CM (W_{CM}) and the springs at CS and CP (W_{CS} and W_{CP}, respectively).

Finally, we remark the common occurrence of diatomite (''farina fossile'' in Italian), i.e. pure white sediments consisting of silica-rich fossil shells of diatoms (main deposits in Fig. 1); actually, there are no evident chronological-genetic relationships between bolar earths and diatomite, but they are often spatially associated.

For sake of simplicity, we will use the term ''bolar earths'' for all CM, CS and CP samples, even for the goethite-poor ones.

Analytical methods

Chemical and mineralogical analyses were performed at the Dipartimento di Scienze della Terra, University of Siena. Mineral phases have been determined by X-ray powder diffraction (XRPD), using an automated Philips PW1710 Bragg-Brentano diffractometer equipped with post-diffraction monochromator, CuKα radiation (λ = 1.5418 Å), from 5° to 70° 2θ (0.04 2θ step size and 2 s time per step).

Whole-rock chemical analyses were obtained by a Philips PW1414 X-ray fluorescence (XRF) spectrometer on 7 g pressed-powders, using international XRF standards. Major elements data were integrated by loss of ignition (LOI) determinations; total iron expressed as Fe_2O_3 wt%.

Scanning electron microscopy (SEM) was performed using a Philips XL30, operating at 20 kV and equipped with an EDAX-DX4 energy dispersive spectrometer (EDS). SEM observations have been obtained both in secondary electrons and in back-scattered electrons (BSE) on powders and filtered flocs, deposited on supporting stubs and homogeneously covering the stub surface. EDS analyses (counting rates close to 2,000–2,500 cps) were performed using a beam raster 50 × 50 μm wide, thus reproducing whole-rock compositions, comparable with XRF data. Raw data were corrected using ZAF approach.

Transmission electron microscopy (TEM) has been carried out by a JEOL 2010 microscope, working at

200 kV, with LaB_6 source, ultra-high resolution pole pieces and 0.19 nm point resolution. The microscope is equipped with an ultra-thin window EDS (ISIS Oxford). TEM–EDS analyses were obtained using large beam spots (approximately 100 nm in diameter), and counting rate between 500 and 1,000 cps; EDS data were treated according to Cliff and Lorimer (1975) and Mellini and Menichini (1985), using standardized J factors. TEM specimens were prepared by depositing the powders on Cu mesh grids, previously covered by a carbon film.

pH and Eh values have been measured by an Eutech Instruments pH-meter (XS pH 6) in waters (in situ) and solids, using a Hamilton ORP electrode. Measurements of pH and Eh in solid samples were obtained following the method described by Mascaro et al. (2001); in particular, fixed aliquots of solid samples were mixed with deionized water at the 1–2.5 weight ratio; pH of the supernatant solution was measured after 20 min centrifugation.

Results

Mineral phases by XRPD

Table 1 reports the XRPD data for CM, CS and CP samples, always consisting of goethite with minor sheet silicates. In particular, CM and CS samples correspond to almost pure goethite, with minor siderite and sheet silicates. In contrast, CP samples reveal large amounts of quartz, sheet silicates (biotite) and feldspars, associated with minor goethite; this evidence confirms that, at least today, the CP deposit is highly contaminated by other sediments, arising from the nearby trachydacite complex.

Whereas the diffraction peaks of siderite, quartz and sheet silicates are narrow, those of goethite are always broad, suggesting a constant low crystallinity, independently from sampling site. Mean crystal size of goethite has been determined by the Scherrer formula $MCS = K\lambda/b_{hkl} \cos \theta_{hkl}$ (where λ = X-ray wavelength, b = full width at half maximum for the diffraction peak at θ; K = shape factor, assumed to be 0.91), measuring the three most intense reflections of goethite (i.e. 1 1 0, 1 1 1 and 2 2 1). Crystal size estimates are reported in Table 2 for five representative CM, CP and CS samples. Mean crystal size is constant from deposit to deposit, ranging from 9 to 17 nm, with recurrent values of 11–13 nm; size determinations on the basis of reflection 2 2 1 could be slightly biased, due to low intensity and poor peak/background ratio.

Table 1 Mineral phases in CM, CS and CP bolar earths from XRPD data

	Goethite	Siderite	Sheet silicates	Quartz	Na, K-feldspars
CM1	××		Traces		
CM2	×	×	×		
CM3	××		×		
CS1	××	××	Traces		
CS2	×		Traces		
CS3	×××		Traces		
CP1	××		××	×	
CP2	×		××	×××	××
CP3	×		×××	×××	××

Chemical compositions of bolar earths and filtered flocs

Bolar earths

Table 3 reports bolar earths compositions, as obtained by XRF and SEM–EDS (average values of at least four 50 × 50 μm raster analyses). Specimens mostly consist of Fe_2O_3 or SiO_2, in variable amounts, from almost pure iron-rich (e.g. CS1) to silica-rich compositions (e.g. CM2). In agreement with XRPD data, iron-rich samples consist of abundant goethite (and possible siderite, as in the case of CS1), whereas there are no relationships between silica contents and quartz, suggesting the occurrence of amorphous silica (expected to be particularly abundant in sample CM2).

Minor, variable amounts of Al_2O_3 depend on the possible occurrence of minerals other than goethite and quartz; for instance, all CP samples are systematically characterized by high Al_2O_3 contents, in agreement with XRPD revealing sheet silicates and feldspars.

Arsenic has been detected in samples from CM (up to 7.4 wt% As_2O_5 in CM1), in CS3, whereas it has not been revealed in the CP samples. Thus, arsenic appears to be heterogeneously distributed among the different deposits and also within the same deposition site, as in the case of the CM quarry, where As-poor samples coexist with the As-richest ones. Chemical data are in agreement with pioneer determinations by Manasse (1915), performed on yellow-dark and brown CM and CS bolar earths (from 0.6 to 9.0 wt% and up to 1.5 wt% As_2O_5, respectively). As a general trend, iron-rich bolar earths are As-enriched as compared to the silica-rich ones.

Filtered flocs

Flocs obtained by filtering of selected water samples (W_{B1} and W_{B2} from Bagnoli; W_{CP1} and W_{CP2} from

Table 2 Mean crystal size (nm) of goethite in CM, CS and CP samples, as determined by Scherrer formula

	Reflections		
	1 1 0	1 1 1	2 2 1
CM1	12	13	13
CM3	9	11	15
CS1	11	11	10
CS3	12	11	13
CP1	12	13	17

Cava del Pino) have been analysed by SEM–EDS (Table 4; average data on at least five analyses for each sample, obtained following the same procedures used for solid bolar earths). W_B flocs have constant compositions, mostly consisting of Fe_2O_3 and SiO_2, with mean values of 61.6–66.9 and 26.3–26.9 wt%, respectively; in contrast W_{CP} flocs have more variable, complex compositions, characterized by the systematic occurrence of Al_2O_3, in agreement with CP bolar earths composition. Arsenic has been detected in W_B (up to 1.9 wt% As_2O_5), whereas it is absent in W_{CP} waters.

Scanning electron microscopy–BSE observations reveal that W_B flocs mostly consist of fine aggregates of iron-rich tiny fibres. Furthermore, we remark the common occurrence of diatoms shells associated with the iron-rich fibres (Fig. 2), possibly suggesting present-day diatomite deposition.

Distribution of As at the nanoscale

Transmission electron microscopy investigation has been performed on selected As-bearing samples from CM and CS, in order to determine the actual size of goethite crystals, the possible occurrence of minor As phases (undetected by XRPD and SEM–EDS) and the nanotextural–nanochemical relationships between goethite crystals and As distribution.

Samples consist of a fine, poorly crystalline association of pseudo-spherical goethite nanocrystals, amorphous silica and minor sheet silicates, in variable amounts. Goethite nanocrystals range from 5 to 20 nm and from 10 to 40 nm in size (samples CS3 and CM1, respectively); they can be isolated (even if closely associated, as in Fig. 3a) or coalesce, giving rise to elongated, rod-shaped particles up to 60 nm (Fig. 3b). Rounded isolated and rod-shaped particles may coexist in the same sample.

Selected area (e.g. Fig. 4, sample CM1) and nanobeam electron diffractions give weak, diffuse, ring-shaped patterns, with *d*-spacings typical of goethite (most intense reflections at 4.2, 2.4 and 1.7 Å, corresponding to d_{110}, d_{111} and d_{221}; arrows in Fig. 4); dif-

Table 3 X-ray fluorescence and SEM–EDS compositions (wt% oxides) of CM, CS and CP bolar earths; XRF As_2O_5 values in ppm

	CM1	CM2	CM3	CS1	CS2	CS3	CP1	CP2	CP3
XRF									
Na_2O	0.1	0.0	0.4	0.0	0.0	0.0	0.2	0.2	0.2
MgO	0.5	0.0	0.7	0.1	0.3	0.0	0.4	0.5	0.5
Al_2O_3	0.6	0.4	8.9	0.7	1.0	0.6	6.3	6.3	8.1
SiO_2	16.9	81.6	36.4	2.1	47.1	6.8	31.4	30.5	35.5
P_2O_5	0.2	0.0	0.1	0.0	0.0	0.2	0.2	0.1	0.1
K_2O	0.1	0.0	2.1	0.0	0.0	0.0	1.4	1.3	1.6
CaO	1.0	0.1	0.9	1.1	1.5	0.1	0.4	0.4	0.4
TiO_2	0.0	0.0	0.6	0.0	0.0	0.0	0.4	0.5	0.6
MnO	0.1	0.0	0.1	0.1	0.0	0.1	0.0	0.1	0.0
$Fe_2O_{3(tot)}$	71.3	13.0	43.1	80.3	44.4	80.0	51.4	53.4	46.1
LOI	9.3	4.8	6.8	15.6	5.7	12.2	7.9	6.7	6.9
As_2O_5 (ppm)	10,942	499	1,601	33	145	1,236	599	619	480
SEM–EDS									
Na_2O	–	–	1.5 (0.4)	–	–	–	–	–	–
MgO		–	0.9 (0.3)	0.9 (0.6)	1.0 (0.1)	0.6 (0.2)	–	1.5 (0.1)	1.5 (0.2)
Al_2O_3	1.0 (0.4)	0.3 (0.1)	14.0 (0.8)	2.3 (0.8)	2.4 (0.4)	1.6 (0.2)	1.7 (0.5)	4.8 (1.4)	10.3 (2.1)
SiO_2	22.0 (0.4)	90.9 (2.5)	47.4 (1.4)	8.3 (0.7)	57.3 (1.5)	15.2 (0.1)	22.4 (7.6)	21.5 (3.1)	38.2 (6.5)
SO_3	–	–	–	–	–	–	0.8 (0.2)	1.0 (0.2)	1.2 (0.3)
K_2O	0.4 (0.1)	–	6.0 (0.2)	0.1 (0.1)	–	–	–	0.5 (0.2)	1.5 (0.4)
CaO	1.4 (0.3)	0.2 (0.1)	–	1.2 (0.3)	1.5 (0.1)	–	–	0.4 (0.2)	0.5 (0.1)
MnO	–	–	–	0.4 (0.2)	–	–	–	–	–
$Fe_2O_{3(tot)}$	68.7 (2.8)	8.6 (1.5)	31.2 (1.6)	87.8 (2.1)	38.8 (1.9)	81.9 (0.3)	75.1 (8.2)	71.9 (4.8)	48.3 (8.9)
As_2O_5	6.5 (1.3)	–	1.4 (0.4)	–	–	1.3 (0.3)	–	–	–

SEM–EDS data are average values over at least four 50 × 50 mm raster analyses; standard deviations are reported in brackets

Table 4 SEM–EDS average analyses (wt% oxides) on filtered flocs from the Bagnoli springs (W_{B1} and W_{B2}) and Il Pino springs (W_{CP1} and W_{CP2})

	W_{B1}	W_{B2}	W_{CP1}	W_{CP2}
Na_2O			0.8	
MgO			6.3	
Al_2O_3	0.8	7.1	11.3	4.8
SiO_2	26.9	26.3	38.3	15.2
SO_3	0.5			10.3
P_2O_5	1.3	3.0		
K_2O			4.0	0.3
CaO	1.6	0.8	1.4	0.3
TiO_2			2.2	
MnO			0.3	
$Fe_2O_{3(tot)}$	66.9	61.6	36.2	69.1
As_2O_5	1.6	1.3	0.0	0.0

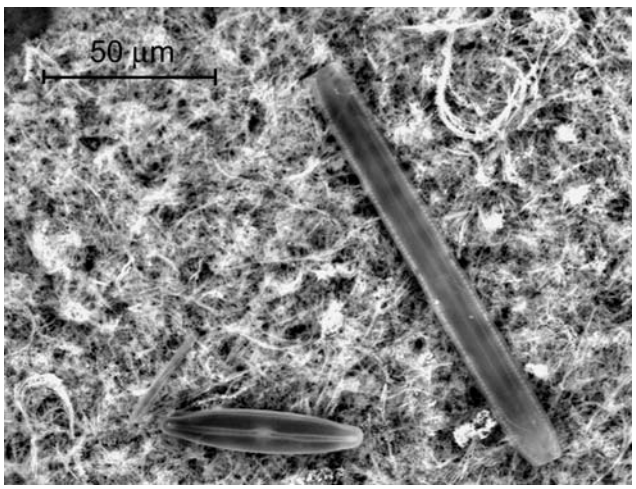

Fig. 2 SEM–BSE image of filtered flocs from the Bagnoli spring. Two elongated diatoms shells are associated to Fe-rich tiny fibres

fraction patterns indicate low crystallinity, independently from sampling site and whole-rock composition. Figure 5a, b shows randomly oriented, rounded nanocrystals of goethite, with regular lattice fringes (samples CS3 and CM1, respectively); nanocrystals are homogeneous, without inner contrast.

TEM–EDS data for CM and CS samples (Table 5) confirm the chemical trends observed by XRF and SEM–EDS, revealing Fe_2O_3 and SiO_2 as the main components. Arsenic is abundant in CM1 (average value 4.8 wt% As_2O_5, up to 8.1 wt%), whereas it occurs in lesser amounts in CS samples (from below detection limit to 4.0 wt% As_2O_5; mean value 1.1 wt%).

Finally, TEM observations revealed that arsenic is strictly associated with goethite nanocrystals, whereas it is absent in the coexisting amorphous silica; X-ray maps performed on nanosized goethite aggregates show perfectly matching Fe and As distributions (Fig. 6). No specific As-phase has been detected.

pH, Eh and temperature measurements

Table 6 reports pH and Eh data for CM, CS and CP bolar earths as well as for water samples at CM, CS, CP and Bagnoli. As regards pH determinations, all solid samples gave similar results, ranging from 4.2 to 8.0, with slight differences from deposit to deposit. In particular, CS samples display a higher variability (from 4.7 to 8.0) than the CM ones (6.0–6.7), whereas CP samples give the lowest pH values. Eh measurements range from 250 to 400 mV, increasing with solution acidity.

Temperature, pH and Eh were also measured in situ in waters at CM, CS, CP and Bagnoli (Table 6). All water samples are close to neutral conditions (6.5–7.7 pH), with constant temperature of 19–21°C; W_{B1}, W_{CS} and W_{CP} are slightly more acidic (pH = 6.5–6.7) than W_{CM}. Eh measurements show slightly negative values for spring waters (ranging from –8 to –30 mV), whereas positive values have been obtained for W_{CM} stream water (194 mV).

pH and temperature measurements at Bagnoli and Il Pino match previous data by Minissale et al. (1997), suggesting poorly variable conditions through time; in contrast, Eh values (–10 mV for W_{B1}, –8 mV for W_{B2} and –10 mV for W_{CP}) deviate from reference data (203 and 303 mV, respectively).

Discussion and conclusions

Goethite crystal size and As adsorption

Crystal size is one of the most critical parameter in determining kinetic and thermodynamic behaviour of minerals (e.g. reaction mechanisms and rates in the case of dissolution, dehydroxilation, interaction with sorbents and solutions); the smaller the crystal size, the higher the specific surface area and the higher the phase reactivity. This feature is of particular interest in the case of goethite, whose surface represents a highly reactive site for adsorption processes. A survey on 256 natural goethites indicates mean crystal size of 15–20 nm (Cornell and Schwertmann 2003), with estimated specific surface area ranging from 80 to 200 m^2/g.

Bolar earths from Mt Amiata consist of goethite crystals, typically 10–15 nm in size, matching the values reported for other natural occurrences. Crystal size determinations based on XRPD and TEM are slightly different (i.e. 9–17 nm vs. 5–40 nm, respectively), due to obvious differences in the two analytical approaches; in particular, XRPD estimations correspond to the actual size of coherent diffracting domains, whereas

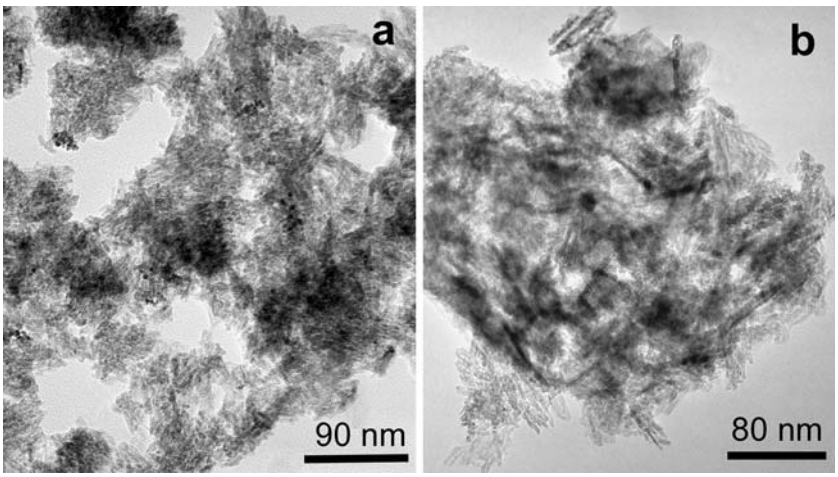

Fig. 3 Transmission electron microscopy images of sample CM1, showing closely associated, but isolated goethite nanocrystals (**a**) vs. coalescent nanocrystals producing elongated, rod-shaped particles (**b**)

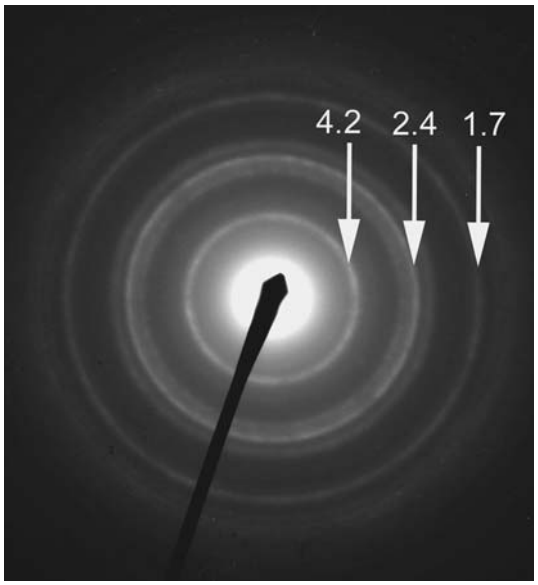

Fig. 4 Ring-shaped SAED pattern of goethite nanocrystals in sample CM1; *arrows* show the three most intense reflections of goethite (corresponding to d_{110}, d_{111} and d_{221})

TEM may reveal larger grain size, possibly resulting from nanocrystals coalescence. Anyway, bolar earths goethites are expected to have high specific surface area (in the 80–200 m^2/g range) and high reactivity for generic ions over several surface functional groups.

The goethite/water interface is commonly represented as a hydroxyl layer, that, depending on pH conditions, can protonate or deprotonate, forming surface complexes with metals and ligands. When pH is lower than pzc (point of zero charge), the surface results in a net positive surface charge, whereas when it is higher, the surface results in a net negative surface charge. Experimental studies on natural and synthetic goethites indicate pzc of 9.0–9.3 pH (Antelo et al. 2005); lower values (between 7.5 and 9 pH) have been recorded only for goethites contaminated by carbonates or other anions (Lumsdon and Evans 1994). Thus, in most common natural systems, goethite surfaces are expected to bind anions rather than positive ions.

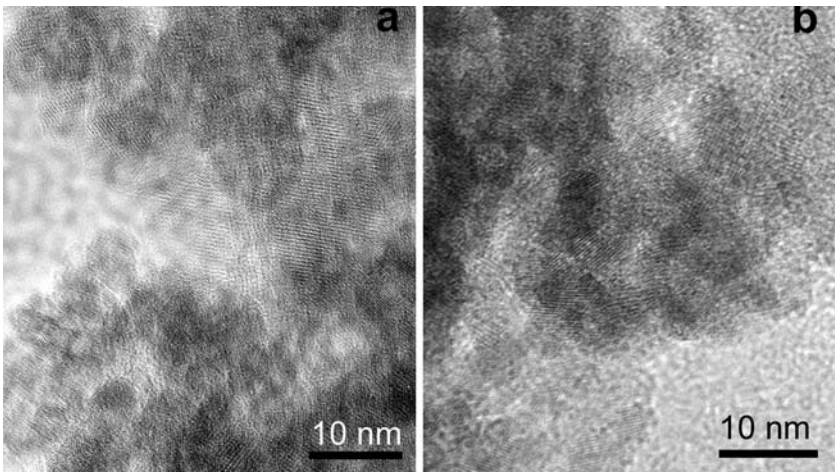

Fig. 5 Transmission electron microscopy lattice images of randomly oriented goethite nanocrystals in sample CS3 (**a**) and CM1 (**b**)

Table 5 TEM–EDS average analyses on CM1, CS1, CS2 and CS3 samples

	CM1	CS1	CS2	CS3
Al_2O_3	–	1.1	0.5	–
SiO_2	16.5	5.8	45.7	11.5
CaO	2.4	0.9	1.3	0.5
$Fe_2O_{3(tot)}$	76.3	93.3	51.9	87.6
As_2O_5	4.8	0.0	1.1	0.5

Table 6 pH, Eh and temperature measurements of bolar earths and waters

	Bolar earths	pH	Eh		Waters	pH	Eh	*T* (°C)
1	CM1	6.5	285	a	W_{CM}	7.7	194	20
2	CM2	6.7	300	b	W_{CS}	6.7	–30	21
3	CM3	6.0	320	c	W_{CP}	6.5	–10	19
4	CS1	8.0	250					
5	CS2	6.0	290	d	W_{B1}	6.5	–10	21
6	CS3	4.7	350	e	W_{B2}	6.9	–8	21
7	CP1	5.6	375					
8	CP2	4.2	400	f	Il Pino[a]	6.7	303	16
9	CP3	4.4	400	g	Bagnoli[a]	6.8	203	21

Numbers and letters (in columns 1 and 5) reported in Fig. 7

[a] Data adapted from Minissale et al. (1997)

pH also affects the kind of As species occurring in the solution (usually, AsO_4^{3-}, $HAsO_4^{2-}$, $H_2AsO_4^-$ and $H_3AsO_4^0$). Experimental models (Smedley and Kinniburgh 2002; Garcia-Sanchez et al. 2002) indicate that, under oxidizing conditions and for pH between 2 and 6, $H_2AsO_4^-$ is the stable form in aqueous solutions, while the anion $HAsO_4^{2-}$ occurs at higher pH (between 7 and 11); for pH between 6 and 8, both species may coexist, whereas H_3AsO_4 and AsO_4^{3-} occur only in extremely acidic and alkaline conditions, respectively (Fig. 7, modified from Smedley and Kinniburgh 2002). Figure 7 also reports Eh and pH measurements for bolar earths and water samples from CM, CS, CP and Bagnoli, suggesting that in CM, CS and CP bolar earths and CM stream waters, As is able to bind to goethite surfaces as arsenate anions (both $H_2AsO_4^-$ and $HAsO_4^{2-}$ depending on pH value). In contrast, Eh values for waters collected immediately close to the spring outflows (Bagnoli, CS and CP) are slightly lower than those for corresponding solid samples and stream waters, possibly suggesting the local occurrence of neutral $H_3AsO_3^0$ in the solution. In this neutral form, arsenic (III) might be mobilized, representing a possible risk for the environmental system. However, Eh values reported by Minissale et al. (1997) for Bagnoli and Il Pino sites (203 and 303 mV, respectively), suggest that the occurrence of neutral $H_3AsO_3^0$ in the solution is time- and space-limited, thus allowing the As(III)–As(V) transformation.

Arsenate adsorption may also have influenced goethite crystal size, favouring the flocculation of nano-sized particles. In fact, the adsorption of arsenate anions on the positively charged goethite surfaces may result into a poisoning effect, leading to negatively charged outer shells capable of inhibiting further outward growth of goethite.

Competitive anions, As desorption behaviour and arsenate stability

Positively charged goethite surfaces may also adsorb anions different from arsenate, thus giving rise to a competitive adsorption process. For instance, phosphate strongly competes with arsenate because of similar binding behaviour of PO_4^{3-}; phosphate adsorption has been described as a faster process, but arsenate adsorption seems to be stronger (Grossl et al. 1997; O'Reilly et al. 2001; Gao and Mucci 2001). Arsenic adsorption to iron hydroxides may also be hampered by other competitive substances typical of

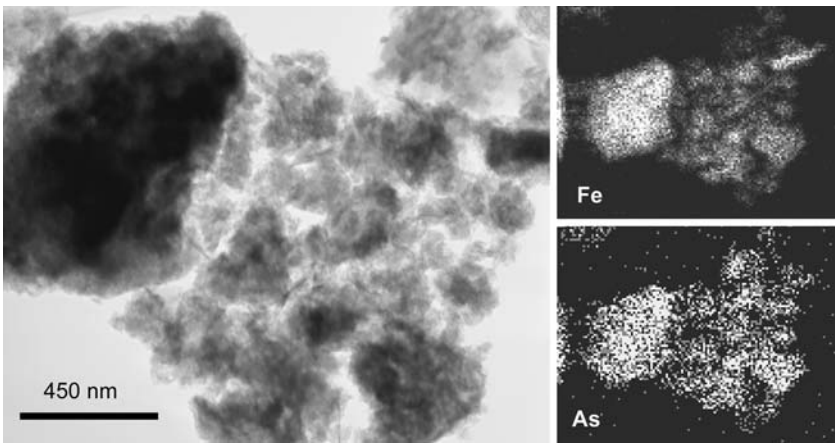

Fig. 6 X-ray maps of Fe and As in goethite aggregates (sample CM1); note the perfectly matching distribution of Fe and As

natural soils, such as aqueous silica, alumina and soluble organic matter (humic, fulvic and citric acids; Gräfe et al. 2001).

The high As amounts in bolar earths suggest substantial absence of strong competitive anions in the depositing aqueous solutions, despite the observed occurrence of abundant amorphous silica, reasonably co-precipitated with goethite. Thus, we may conclude that, at least under the physical/chemical conditions at which bolar earths precipitated, silica was less competitive than arsenate, in terms of adsorption on goethite surface.

Once adsorbed on goethite surface, arsenate is not easily desorbed or removed, unless pH conditions severely change. Experimental studies on arsenate adsorption and desorption kinetics in goethites at pH 4 and 6 (O'Reilly et al. 2001) show that the surface complex is very stable for extended time. Hence, under the observed aerobic and acidic to near-neutral conditions (pH from 4.2 to 8, as reported in Fig. 7), arsenate adsorption on goethite is expected to be stable, suggesting low risk for arsenic desorption; bolar earths thus represent an example of natural self-remediating, stable As-trap.

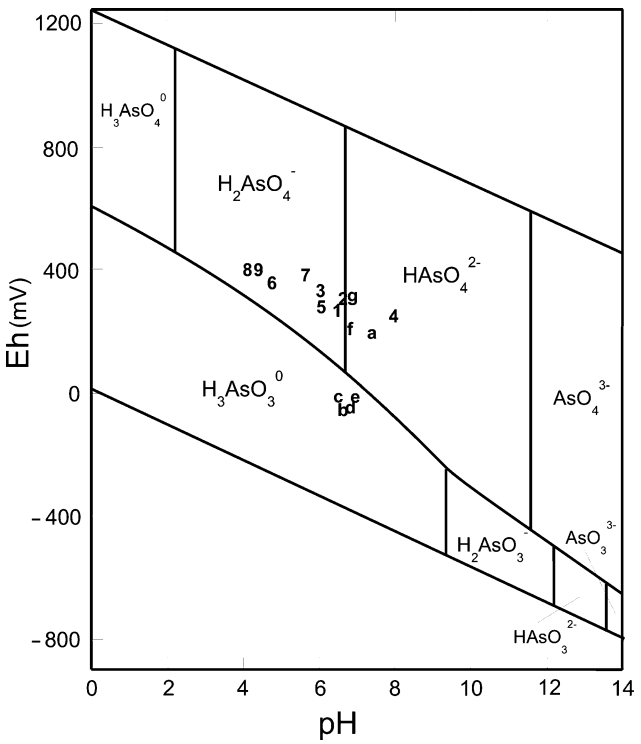

Fig. 7 Eh vs. pH diagram (modified from Smedley and Kinniburgh 2002) with data for CM, CS, CP solid samples and for water samples from CM, CS, CP and Bagnoli springs (*numbers* and *letters* as in Table 6)

Nature of bolar earths depositing fluids and possible present-day deposition site of As-rich goethite

Bolar earths consist of As-rich goethites often intermixed to amorphous silica; accordingly, they should have been formed by precipitation from iron-silica rich fluids (Lotti 1910; Manasse 1915), characterized by relatively high As contents. Slight variations in physical/chemical parameters of fluids could have favoured pure goethite or goethite + silica precipitation.

The origin of these iron-silica rich fluids is quite uncertain, due to the chemical variability of hydrothermal fluids and to the possible mixing with meteoric waters. Minissale et al. (1997) reported three main geological reservoirs in the Mt Amiata region, characterized by low Fe content and Ca–HCO_3, Ca–SO_4 or Na–Cl rich compositions; most thermal and cold springs in the area are consistent with these compositions. Thus, the occurrence of Fe-rich fluids should be related to time-limited episodes, to locally different geological reservoirs or to specific physico-chemical processes, involving local dissolution of country rocks by slightly acidic waters (Minissale et al. 1997).

Actually, Fe-rich solutions may locally occur (e.g. the cold springs at Putizza Rondinaia and Galleria Nuova Italia; Minissale et al. 1997), but they are As-free. At present, the only probable site for As-rich goethite deposition is represented by the Bagnoli cold springs, characterized by As content of 0.036 mg/l, high Si + Fe and low HCO_3 + Ca compositions, sharply differing from other nearby geothermal sources (Minissale et al. 1997). This hypothesis is confirmed by the presence of As in the Fe-rich filtered flocs from W_B (up to 1.9 wt% As_2O_5).

Acknowledgement The present research has been funded by the PRIN 2004 project on "Mineralogia delle fasi responsabili della mobilizzazione e rimozione dell'arsenico: implicazioni ambientali."

References

Antelo J, Avena M, Fiol S, López R, Arce F (2005) Effects of pH and ionic strength on the adsorption of phosphate and arsenate at the goethite–water interface. J Colloid Interface Sci 285:476–486

Brogi A (2004) Miocene low-angle detachments and upper crust megaboudinage in the Mt. Amiata geothermal area (Northern Apennines, Italy). Geodin Acta 17(6):375–387

Carlson L, Bigham JM, Schwertmann U, Kyek A, Wagner F (2002) Scavenging of As from acid mine drainage by schwertmannite and ferrihydrite: a comparison with synthetic analogues. Environ Sci Technol 36:1712–1719

Cliff G, Lorimer GW (1975) The quantitative analysis of thin specimens. J Microsc 103:203–207

Cornell RM, Schwertmann U (2003) The iron oxides. Structure, properties, reactions, occurrence and uses, 2nd edn. Wiley, Weinheim, Germany, p 663

Cuteri F, Mascaro I (1995) Colline metallifere. Inventario del patrimonio minerario e mineralogico. In: Regione Toscana (ed) Aspetti naturalistici e storico-archeologici, vol 1. Firenze p 182

Dixit S, Hering J (2003) Comparison of arsenic (V) and arsenic (III) sorption onto iron oxide minerals: implications for arsenic mobility. Environ Sci Technol 37:4182–4189

Dzombak DA, Morel FM (1990) Surface complexation modelling: hydrous ferric oxide. Wiley, New York

Fendorf S, Eick M, Grossl P, Sparks D (1997) Arsenate and chromate retention mechanism on goethite. 1. Surface structure. Environ Sci Technol 31:315–320

Ferrari L, Ponticelli S, Burlamacchi L, Manetti P (1996) Volcanological evolution of the Monte Amiata, southern Tuscany: new geological and petrochemical data. Acta Vulcanol 8:41–56

Gao Y, Mucci A (2001) Acid base reactions, phosphate and arsenate complexation, and their competitive adsorption at the surface of goethite in 0.7 M NaCl solution. Geochim Cosmochim Acta 65:2361–2378

Garcia-Sanchez A, Alvarez-Ayuso E, Rodriguez-Martin F (2002) Sorption of As (V) by some oxyhydroxides and clay minerals. Application to its immobilization in two polluted mining soils. Clay Miner 37:187–194

Gräfe M, Eick MJ, Grossl PR (2001) Adsorption of arsenate (V) and arsenite (III) on goethite in the presence and absence of dissolved organic carbon. Soil Sci Soc Am J 65(6):1680–1687

Grossl PR, Eick M, Sparks DL, Goldberg S, Ainsworth CC (1997) Arsenate and chromate retention mechanisms on goethite. 2. Kinetic evaluation using a pressure-jump relaxation technique. Environ Sci Technol 31:321–326

Hiemstra T, Van Riemsdijk WH (1999) Surface structural ion adsorption modelling of competitive binding of oxyanions by metal (hydr)oxides. J Colloid Interface Sci 210:182–193

Loppi S (2000) Lichen biomonitoring as a tool for assessing air quality in geothermal areas. In: Iglesis E, Blackwell D, Hunt T, Kund J, Tamanyu S, Kimbara K (eds) Proceedings of the World geothermal congress 2000, Kyushu-Tohoku, Japan

Lotti B (1910) Geologia della Toscana. Mem Descr Carta Geol Ital XIII:482

Lumsdon DO, Evans LJ (1994) Surface complexation model parameters for goethite (FeOOH). J Colloid Interface Sci 164:119–125

Manasse E (1915) Sulla composizione chimica delle terre gialle e bolari del Monte Amiata. Atti Soc Tosc Sci Nat Mem 30:101–119

Manasse A, Mellini M (2006) Iron (hydr)oxide nanocrystals in raw and burnt sienna pigments. Eur J Mineral (in press)

Manning BA, Fendorf SE, Goldberg S (1998) Surface structures and stability of arsenic (III) on goethite: spectroscopic evidence for inner-sphere complexes. Environ Sci Technol 32:2383–2388

Mantelli F, Salutini A, Grilli Ciclioni A, Bucci P, Carrozzino S, Bozzelli M (1999) Presenza di arsenico nelle acque di acquedotto e nelle fonti di approvvigionamento idrico in Toscana. Quaderni di Geologia Applicata 2:271–281

Mascaro I, Benvenuti M, Corsini F, Costagliola P, Lattanzi P, Parrini P, Tanelli G (2001) Mine wastes at the polymetallic deposit of Fenice Capanne (southern Tuscany, Italy). Mineralogy, geochemistry and environmental impact. Environ Geol 41:417–429

Mellini M, Menichini R (1985) Proportionality factors for thin film TEM/EDS microanalysis of silicate minerals. Rend Soc Ital Mineral Petrol 40:261–266

Minissale A, Magro G, Vaselli O, Verrucchi C, Perticone I (1997) Geochemistry of water and gas discharges from the Mt. Amiata silicic complex and surrounding areas (Central Italy). J Volcanol Geotherm Res 79:223–251

O'Reilly SE, Strawn DG, Sparks DL (2001) Residence time effects on arsenate adsorption/desorption mechanisms on goethite. Soil Sci Soc Am J 65:67–77

Protano G, Riccobono F, Sabatini G (1998) Geochemical maps of Southern Tuscany. Construction criteria and environmental relevance through the Hg, As, S, Pb, Cd examples. Mem Descr Carta Geol Ital LV:109–140

Sherman DM, Randall SR (2003) Surface complexation of arsenic (V) to iron (III) (hydr)oxides: structural mechanism from ab initio molecular geometries and EXAFS spectroscopy. Geochim Cosmochim Acta 67:4223–4230

Smedley PL, Kinniburgh DG (2002) A review of the source, behaviour and distribution of arsenic in natural waters. Appl Geochem 17:517–568

Sun X, Doner HE (1996) An investigation of arsenate and arsenite bonding structures on goethite by FTIR. Soil Sci 161:865–872

Tamasi G, Cini R (2004) Heavy metals in drinking waters from Mount Amiata (Tuscany, Italy). Possible risks from arsenic for public health in the Province of Siena. Sci Total Environ 327:41–51

Waychunas GA, Davis JA, Fuller CC (1995) Geometry of sorbed arsenate on ferrihydrite and crystalline FeOOH: reevaluation of EXAFS results and topological factors in prediction sorbate geometry and evidence for monodentate complexes. Geochim Cosmochim Acta 59:3655–3661

Webster JG, Nordstrom DK (2003) Geothermal arsenic—the source, transport and fate of arsenic in geothermal systems. In: Welch AH, Stollwerk KG (eds) Arsenic in groundwater. Kluwer Academic Publishers, Boston, pp 101–125